



Fall detection and human activity classification using wearable sensors and compressed sensing

Oussama Kerdjidi^{1,2} · Naeem Ramzan³ · Khalida Ghanem² · Abbes Amira³ · Fatima Chouireb¹

Received: 20 May 2018 / Accepted: 14 January 2019
© Springer-Verlag GmbH Germany, part of Springer Nature 2019

Abstract

The fall of elderly patients is still a critical medical issue since it can cause irreversible bone injuries due to the elderly bones weakness. To mitigate the likelihood of the occurrence of a fall, continuously tracking the patients with balance and health issues has been envisaged, despite being unpractical. To address this problem, we propose an efficient automatic fall detection system which is also fitted for the detection of different activities of daily living (ADL). The system relies on a wearable Shimmer device, to transmit some inertial signals via a wireless connection to a computer. Aiming at reducing the size of the transmitted data and minimizing the energy consumption, a compressive sensing (CS) method is applied. In this perspective, we started by creating our dataset from 17 subjects performing a set of movements, then three distinct systems were investigated: one which detects the presence or the absence of the fall, a second which detects static or dynamic movements including the fall, and a third which recognizes the fall and six other ADL activities. In the acquisition and classification steps, first only the data collected by the accelerometer are exploited, then a mixture of the accelerometer and gyroscope measurements are taken into consideration. The two configurations are compared and the resulting system incorporating CS capabilities is shown to achieve up to 99.8% of accuracy.

Keywords Fall detection · Human activity · Wearable sensors · Compressed sensing · Classification

1 Introduction

One of the major problems the current societies have to face, is the aging and the lack of physical activity of their population. These two factors (age and non activity) are behind disastrous fall accidents, which take place indoors or outdoors. Various statistical studies stated that falls are the principal cause of hospitalizations for injuries (Sherrington Catherine 2017), and recent reports show that 30% of people, at the age of 65 or over, have the highest risk of falling (Lusardi 2017). This has led to an increased number of interventions for securing or aiding this category of population. To

consolidate these efforts, research interest has also been oriented towards the investigation of technical solutions to rescue/save people's life. Under this umbrella, the development of technology and the miniaturization of electronic devices which can collect health data, have enabled the design/deployment of applications, such as fall detection or health monitoring (Sheltami et al 2016; Vallabh and Malekian 2018). A fall detection system, for instance, allows to prevent the elderly subjects fractures, and sends an alarm to the nearby hospital, thereby allowing timely intervention, to provide a first aid to the patient. Moreover, the system may collect the per day activity of the patients in order to monitor their health's state and progress.

Several approaches have been proposed to identify fall and ADL activities using a multitude of sensors and approaches (Casilari et al 2017; Micucci et al 2017). Li et al (2009) utilized a sample thresholding method between an accelerometer and a gyroscope to detect the fall. Similarly, Lee and Carlisle (2011) applied a two thresholding method to analyze the data acquired from a smartphone and an accelerometers, in order to identify the movements and the different simulated falls. The technique of thresholding has some

✉ Oussama Kerdjidi
kerdjidjoussama@gmail.com

¹ Laboratory of Telecommunications, Signals and Systems, Department of Electronics, University Amar Telidji, Laghouat, Algeria

² Division Télécom, Centre de développement des technologies avancées (CDTA), Algiers, Algeria

³ School of Engineering and Computing, University of the West of Scotland, Paisley, Scotland, UK

limitations; mainly because it generates a great deal of false alarms since it is not able to accurately distinguish between the fall and ADL movements. Some of other approaches resort to the video processing to identify the movements. For instance, in this context, the weight and the height aspect ratio of an individual are evaluated and used, after separating the background from the object of interest (Harrou et al 2017). Litvak et al (2008) combined the extracted features from the floor accelerometer and the microphone measurements to be considered in the classifier. Alternatively, the classification for various classes of movements could be adapted to different types of data (Aslan et al 2015; Daher et al 2017; Ando et al 2016; Makhoul et al 2018). To date, device-free activity recognition has attracted considerable attention. Exploiting the radio signal fluctuations induced by subject's movements to identify the activities has been addressed in (Sigg et al 2013; Han et al 2016; Ruan et al 2016), where Radio-Frequency Identification (RFID) technology is deployed on a large scale to recognize human activities. Hence, it has a shortcoming, it needs to install a lot of sensors on the wall or house, and the oversight in outdoor is also a problem.

In the literature, different types of sensors, with the pertaining processing techniques, have been adopted in the design of a fall detection system. They can be generally categorized into three distinct sets: the wearable sensors, the environmental sensors, and the vision-based detection sensors (Alhimale et al 2014; Mubashir et al 2013; Igual et al 2013). The last type of sensors has received a great deal of research and industry interests, and is usually relying on the using of a sensing device such as cameras, more particularly Microsoft Kinect, as well as computer vision techniques to manipulate and exploit the captured data (Zerrouki et al 2016; Aslan et al 2015; Kwolek and Kepski 2016). Nowadays, this activity detection method enjoys a high efficiency in evaluating the position and the shape of the subject, by exploiting the recent advances in image processing and pattern recognition techniques. However, its main impediments lie in its limited coverage area and inability to track the user out of the range of visibility, its likely subject's privacy violation, and the requirements of deployment of several such cameras for a viable detection. Indeed, for a conventional home, many cameras need to be installed in order to cover the largest possible area, making this approach very expensive.

The second category, which is environmental sensors, targets flooring applications. The main characteristic of these ambient sensor-based systems is that, for the movements tracking, they rely on the environmental metrics for the analysis of the gait and the trajectory of the elderly people (Daher et al 2017; Feng et al 2016; Jekanovic et al 2016; Cheffena 2016). The system identifies the different movements by using the sensors recordings in terms of vibration

of the floor, pressure, sound, infrared rays, etc. This approach does not take into account whether the patient is outdoors or in the area of non-coverage of the sensors. Moreover, in most of the cases, it is necessary to cover the patient's home with a special raised floor, use an important number of sensors with a high resolution, and install them within the floor and along the walls, which may become cost prohibitive.

The third category of systems is an improved version of the environmental type. It is a fact that with the progress in technology, and the decrease of its cost, wearable devices are now commonly used in different areas, such as health applications, sports, entertainments, etc. (Makhoul et al 2018; Ghanem 2013; Hall 2016). Another motivating factor was the fact that research has witnessed a tremendous eagerness for applications on daily activity recognition, which resorts to wearable devices along with efficient processing techniques (Ando et al 2016; Ozcan et al 2017; Gibson et al 2016; Yao et al 2015). Various sensors (accelerometer, gyroscope, magnetometer, camera, etc.) are now wearable, resulting in a sophisticated system which can analyze any information captured by them, whether indoors or outdoors. More interesting, with such systems, there is no area limit for the data collection when the patient moves from a location setting to another. One of the crucial problems with this solution is the battery life. To ensure a long time device operation and a sufficient patient information, the energy consumption has to be minimized.

To address this issue, Gibson et al (2017) proposed a method which relies only on the accelerometer device, and exploits the Compressive Sensing (CS) principle to maintain a viable performance, while reducing wearable device energy consumption. In addition, Cheng et al (2017b) resorted to the same technique of CS to save energy and recognize the human activity, by employing the mobile phone camera. Owing to the involved video data, this system suffers from a high computation complexity. Hui and Zhongmin (2017) suggested using the compressed sensing method for recognizing activities in which both acceleration data and phone placement information are utilized. The authors considered three placements of mobile phones (the hand, trouser pocket, and handbag). In real life, the users may carry their phones in additional different places which may cause the system failure. Yao et al (2018) used the RFID technology to recognize various activities for the independent living persons, where the CS is exploited to learn a dictionary of different movements. According to the authors, the approach has some problems, such as the effect of the distance between the system and the RFID tags, and the environment changes. For their solution, the outdoor may be a big challenge. Zhang et al (2017) adapted the CS for acceleration data transmission in human motion capture. They used as features the correlation between the sparsity and the compression ratio of

acceleration data in a learning phase. Cheng et al (2017c) presents a classification method based on random projections, which can save energy consumption while maintaining a great activity recognition rate. With four subjects, the method may be tested on larger datasets with more human activities and more subjects.

In this paper, we propose a system able to detect a fall and recognize the selected human daily activities, and which resorts to CS capabilities to increase battery life. The system collects real-time data from the accelerometer and the gyroscope sensors, and exploits the dual benefit of both in enhancing the performance of the system. To the best of the authors' knowledge, the only other work on CS-based architecture taking advantage from more than a wearable sensor, is the one reported in (Cheng et al 2017b) which combines the collected data from the camera and the accelerometer. In our proposed architecture, we have opted for a wearable shimmer device to collect cinematic data from subjects. This choice is motivated by the various embedded sensors and the interesting offered features in Shimmer platform, which open an interesting door to the extension of our work in the future (Burns et al 2010a, b). These features include the connectivity, processing, storage and the design robustness capabilities (Burns et al 2010b). Our methodology starts by the collection of the 3-axis linear acceleration and the 3-axis angular velocity signals by the aid of the Shimmer platform, then applying the CS-based processing followed by the adoption of retained classification algorithms. We have created our own database by carrying out these measurements on 17 subjects performing the same set of measurements in the same environment. The resulting system is afterwards investigated according to two criteria, namely the concerned sensors, and the influence of the CS processing in the quality of the detection and the energy reduction. Under the former criteria, the detection efficiencies are compared when separately using accelerometer, gyroscope, and both of them. Similarly, within the latter criteria, the recovery accuracy of Matching Pursuit (MP) and Orthogonal Matching Pursuit (OMP) algorithms are discussed, as well as the impingement of the number of iterations in CS. These two approaches are tested according to three scenarios.

The first scenario, referred to as scenario A, consists of 2 classes (fall and non-fall) where the class of non-fall comprises all the remaining ADL activities except the fall. The second scenario, denoted B, is composed of 3 classes; fall, static and dynamic movements, where the two latter are referred to as non-activity, and activity classes, respectively. The last scenario, called C, aims at recognizing and predicting the different human activities as well as the fall movement. We have selected these three scenarios so that to make the system flexible and adaptive/personalizable to various targeted applications (sports, emergency, health, and activity report).

The rest of this paper is organized as follows. Section 2 describes the data acquisition procedure and details the list and duration of the retained movements. Classical fall detection and activity recognition framework, along with the selected temporal features for classification, are depicted in Sect. 3. Afterwards, the proposed scheme involving CS paradigm using MP and OMP approaches is described. The study is carried out when using each sensor's data separately, and then by merging the data issued from the two sensors. The performances of the two resulting systems under the different scenarios and classifiers are compared and discussed in Sect. 4. Finally, the conclusion is drawn.

2 Data collection

As mentioned earlier, Shimmer platform has been retained for the collection of the signals of interest, because it complies with the requirements of our application, such as being lightweight, easy to wear, and offering a wide range of signals (accelerometer, gyroscope, magnetometer, electrocardiogram (ECG), etc), which may be exploited in our decision making system. However, as any wearable device, Shimmer needs to be recharged regularly, and since it targets mainly healthcare applications, it may be quite critical if its battery becomes very low. Hence, this issue should be seriously taken in charge.

On the other hand, It has been reported in the literature that the best device placement is on the chest (Ozdemir 2016; Ntanas et al 2017). Therefore, we have also placed Shimmer on the chest to carry out our fall detection application, where the accelerometer and the gyroscope sensors have been used to record signals, encompassing both abrupt transitions and signals pertaining to periodic movements. These latter are transferred via Bluetooth to a local repository on a computer, where they are stored and processed.

The measurements involve a group of 17 volunteers, among which 10 males and 7 females, of various ages, heights and weights. Instructions were given to each volunteer to perform falls-like and ADL movements, with the latter including the majority of daily movements, such as lying, sitting, standing, walking, jumping and running. All participants repeated each ADL movement three times between 2.5 and 60 s, whereas the fall movements were repeated several times. In total, each individual performed at least 21 movements with varying durations. Figure 1 illustrates a volunteer during the measurements campaign in the specific environment, while Table 1 summarizes the number of events and the different information of volunteers.

The volunteers perform all movements naturally while observing the same measurements conditions, except for the fall, where it was noted that most of them, more particularly the females, held back despite the presence of

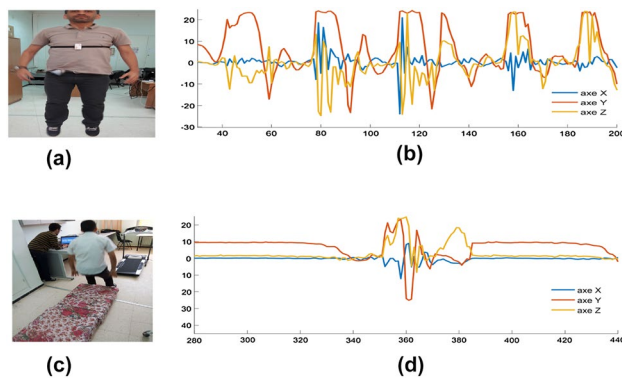


Fig. 1 Activity type examples and experimental collected signals, **a** jump movement, **b** accelerometer signals for jump, **c** fall movement, **d** accelerometer signals for fall

Table 1 Summary of dataset

Number of events	360
Average age	22–45
Genre	10 Male–7 Female
Height	155–183 cm
Weight	55–85 kg
Time record	30–60 s

a mattress to reduce the impact of the fall. Afterwards, the collected signals were organized in seven files, corresponding to the different movements cited previously, and containing the data of the volunteers. In each of the files, six signals pertaining to the relative x, y, and z-dimensions of the accelerations and angular velocities were stored.

3 Proposed framework

An outline of the classical system relying on the acceleration and angular velocity acquisition, is illustrated in Fig. 2a, where the different stages until data exploitation are enumerated, namely, the data acquisition, the features extraction, the classification, the activity identification, and the resulting decision.

Figure 2b gives the proposed alternative architecture for ADL activity recognition/fall detection which relies on the viable characteristics of CS concept. A compromise in the signal size reduction has been observed, by selecting an adequate number of iterations, which ensures a device energy saving, while maintaining a good quality of signal recovery. At the reception side, two reconstruction algorithms are implemented, namely the MP and OMP algorithms, to reconstruct the original signals. A parametric study for the recovery quality is performed by evaluating the performance of the system under different number of iterations. Our previous study investigated the impact of the selection of different CS parameters (Kerdjидj et al 2014).

More explanations about the feature extraction and the CS algorithms are provided in the following subsections.

3.1 Feature extraction

We have relied in the extraction of our features, a critical step for the definition of an accurate machine learning model, on the temporal data acquired from the two sensors. Our choice for a processing in the temporal domain is supported by the relative easiness of temporal computation and implementation on a hardware platform. We have considered in our study feature vectors (FVs) extracted from windows of 128 samples, which corresponds to 2.56 s at the used 50 Hz sampling rate of the device. From this output, depending on

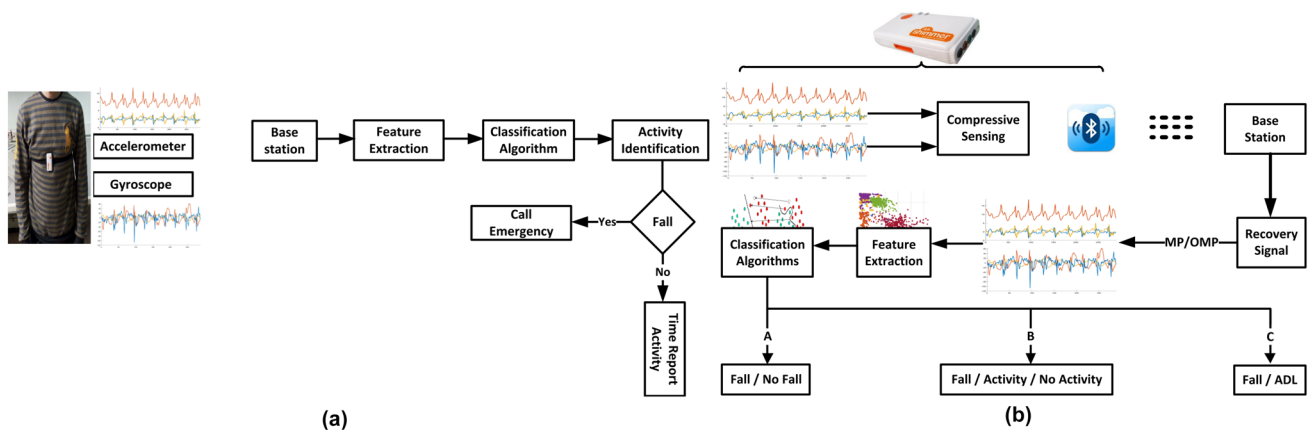


Fig. 2 Proposed method for movement and fall detection, **a** classical system, **b** system including compressive sensing

Table 2 Statistical equation used to extract features

Time Domain	Description
Maximum	$\max(x_i)$
Minimum	$\min(x_i)$
Peak	Number of peak
Mean	$\frac{1}{N} \sum_{i=1}^N x_i$
Signal magnitude vector	$\sqrt{x_i^2 + y_i^2 + z_i^2}$
Standard Deviation	$\sqrt{\frac{1}{N-1} \sum_{i=1}^N (x_i - \mu)^2}$
Root mean square	$\sqrt{\frac{1}{N} \sum_{i=1}^N (x_i)^2}$
Pearson correlation	$\frac{\sum_{i=1}^N (x_i - \bar{x})(y_i - \bar{y})}{\sqrt{\sum_{i=1}^N (x_i - \bar{x})^2} \sqrt{\sum_{i=1}^N (y_i - \bar{y})^2}}$

Table 3 Feature extracted from sensors

Seq_i	The features
Seq_A	max, min, mean, number of peaks, std, and rms
Seq_S	Signal magnitude vector and pearson correlation

the scenario, every fall and ADL movement of 2.56 s generates a FV which is computed from the 6 signals emanating from the accelerometer and the gyroscope, resulting in a total of 44 features contained in each FV. Where, the corresponding statistical equations which have served for their extraction in the time domain are listed in Table 2, where \bar{x} and \bar{y} is the mean of signal x and y , N the length of the signal.

In the construction of the vector FV , two sets of features, referred to as Seq_S and Seq_A , were merged. As seen in Table 3, Seq_S comprises the magnitude vector of the measurements and the three Pearson correlation pertaining to each sensor, which gives in total 8 features. On the other hand, Seq_A consists of the evaluation per axis of each sensor of the average, the number of peaks in which the amplitude is superior or equal to the mean, the maximum, the minimum, the root mean square (RMS) value and the standard deviation (STD), which yields a number of features of 36. Hence, a total of 44 features are gathered.

3.2 Compressive sensing

CS technique has been recently introduced by Donoho (2006), and Candes et al (2006) to open a new perspective for signal recovery from incomplete information, based on

the hypothesis that the signal is sparse in some basis. CS performs two main operations: the compression and the recovery of the signal. The resulting compressed signal of length M could be expressed as:

$$Y = \Theta x \quad (1)$$

where, x is the non-sparse input signal vector with length N , $\Theta = \Phi\Psi$, with Θ being the $M \times N$ sensing matrix, Φ the sensing basis, and Ψ the $N \times N$ sparsifying basis. $M \ll N$ observations are extracted from the N samples through the processing depicted by eq. 1 which could be rewritten as:

$$Y = \Phi f \quad (2)$$

where $f = \Psi x$ is the projection of the original signal on the space generated by the sparsifying matrix.

For a CS algorithm to be efficient, three key conditions are to be met: Firstly, the signal f needs to be sparse in a given domain, secondly the matrix Φ should satisfy the Restricted Isometric Property (RIP), and thirdly the matrices Ψ and Φ are to be incoherent (Candes and Wakin 2008).

3.2.1 Matching pursuit

Mallat and Zhang firstly introduced the MP algorithm in the context of harmonic estimation (Mallat and Zhang 1993). MP is an iterative greedy algorithm which encompasses two phases: the selection and the update. The first module is made up to find the best-correlated atom from the dictionary with the residual current error. The second module's role is to ensure the update operation, by subtracting the previously calculated correlated part from the residue. The algorithm terminates when some criteria are satisfied, or the maximum number of iterations is exceeded. The MP approach is depicted below in algorithm 1.

Algorithm 1 Matching Pursuit

Input: Φ : Sensing matrix ; Y : Observation vector; K : Sparsity of signal X .

Output: \hat{X} : Original signal estimation

Procedure:

- 1: Initialise residual $r_0 = Y$ and set iteration counter $i = 1$.
- 2: Find index $\lambda_i = \arg\max |\langle r_{i-1}, \phi_j \rangle|$ for $j = 1 \dots N$.
- 3: Calculate the new approximation $\hat{X}_i = \hat{X}_{i-1} + \langle \phi_{\lambda_i}, r_{i-1} \rangle \phi_{\lambda_i}$ and the new residual $r_i = Y - \hat{X}_{i-1} = r_{i-1} - \langle \phi_{\lambda_i}, r_{i-1} \rangle \phi_{\lambda_i}$
- 4: Increment iteration counter $i = i + 1$, return to step 2 if $i < K$
- 5: Output estimation \hat{X}

3.2.2 Orthogonal matching pursuit

The OMP algorithm is an improved version of MP by Tropp and Gilbert (2007, 2005), which was developed in order to overcome the impediment experienced by being trapped in the selection of the same atom several times. OMP

algorithm remedies the issue starting by determining the most correlated atom with the current residue, similarly to the MP algorithm, then, unlike the latter, recalculates the estimated signal at each iteration. Therefore, it will never occur that the same vector will be chosen again (step 3 and 4 of algorithm 2). While OMP usually provides a superior performance than MP, its implementation is more complex. Algorithm 2 lists the different steps required with OMP technique. CS is utilized in our system to recover the data collected on the 3 axis x, y, and z of Shimmer sensors, and the approximation of the original signal is retrieved by the aid of MP and OMP algorithms. Depending on the number of iterations involved in these recovery algorithms, the number of resulting samples will be reduced for each sensor (Kerdjadj et al 2014). In each sensor of the device, 3 signals corresponding to the three dimensions x, y, and z, of 128 samples length, are produced, and are recovered after either 20, 30 or 50 iterations.

Algorithm 2 Orthogonal Matching Pursuit

Input: Φ : Sensing matrix ; Y: Observation vector; K: Sparsity of signal X

Output: \hat{X} : Original signal estimation

Procedure:

- 1: Initialise residual $r_0 = Y$ and set iteration counter $i = 1$.
- 2: Find index $\lambda_i = \operatorname{argmax}_j |\langle r_{i-1}, \phi_j \rangle|$ for $j = 1 \dots N$.
- 3: Increase index set $\Lambda_i = \Lambda_{i-1} \cup \{\lambda_i\}$ and matrix column vectors $\Phi_i = [\Phi_{i-1} \ \Phi_{\lambda_i}]$
- 4: Solve least squares problem for estimation \hat{X} of signal X; $\hat{X}_i = \operatorname{argmin} \|Y - \Phi_i \hat{X}_i\|$
- 5: Calculate new residual $r_i = Y - \Phi_i \hat{X}_i$
- 6: Increment iteration counter $i = i + 1$, return to step 2 if $i < K$
- 7: Output estimation \hat{X}

As mentioned earlier, MP and OMP are close since they both imply the using of a selection and an update stages. In the selection phase, the correlation is computed to get the mostly correlated basis vector and the corresponding coefficient of the output signal. Subsequently, the update stage concerns the evaluation of the estimate, which yields the minimum of the norm of the difference between the sensor output signal and the projected value on the found dimensions. Then, the calculation of the residual is carried out, as the distance between the output signal and the projection of the just-found estimate on the gradually-constructed parsifying matrix. Table 4 compares the level of complexity of the used MP and OMP algorithms, where N is the length of the signal, α is a constant which is higher than one, and i is the matrix size. From the Table 4, it can be seen that the two algorithms enjoy a similar level of complexity in the selection phase, whereas in the update counterpart, OMP algorithm needs to perform a higher number of operations. Hence the same performance/complexity dilemma as in any application arises, and one has to choose according to what it is afforded.

Table 4 Complexity order of a given iteration algorithms

	Step	MP	OMP
Selection	Correlations	αN^2	αN^2
	Maximum	αN	αN
Update	Approximation	0	iN
	Coefficients	0	i^2
	Residual	N	iN

After extracting the features enumerated in Table 2, and assigning to each movement the corresponding class according to the chosen scenario, we applied the CS to the new data using MP and OMP algorithms and tested the performance of each classifier after recovery the signal with various iterations. The system is evaluated using four classifiers, namely the k-Nearest Neighbor (k-NN), the Support Vector Machine (SVM), the Decision Tree (DT) and the Ensemble Classifier (EC) (Duda et al 2012).

Based on our future hardware requirement, we considered two different distance functions for the k-NN approach, namely Euclidean (Euc or Fine) and cosine (Cos) ones. Unlike k-NN, SVM requires the training stage to create a model, and we have investigated its performance using the three kernel functions: Linear (Lin), Quadratic (Qua) and Cubic (Cub). DT is a fast algorithm for prediction with less memory usage compared to SVM. In this work, we have used three types of DT: Simple, Medium (Med) and Complex (Com). Finally, we have resorted to EC with its Bagged tree (BT) and Sub-space Discriminant (SD) versions.

4 Results and comparison

For evaluating the system, we consider three scenarios as showcased in Fig. 3. In the scenario (A), the system predicts only two classes, the fall and no-fall occurrences, where, if the classification is accurately performed, ADL movements should be grouped in the no-fall class. The second scenario (B) attempts not only to detect the fall event, but also to record the activity or the no-activity of the patient. For this, the system categorizes as no-activity the following three movements: laying, sitting and standing; while activity class encompasses walking, jumping and running movements. The last system is able to recognize, in addition to the fall event, the six aforementioned movements separately.

Afterwards, the performance of the proposed system, with and without using CS techniques is evaluated using the following classification metrics: the recall, the precision, the specificity and the F1 score. To avoid data over-fitting, 10-fold cross-validation (CV) is used.

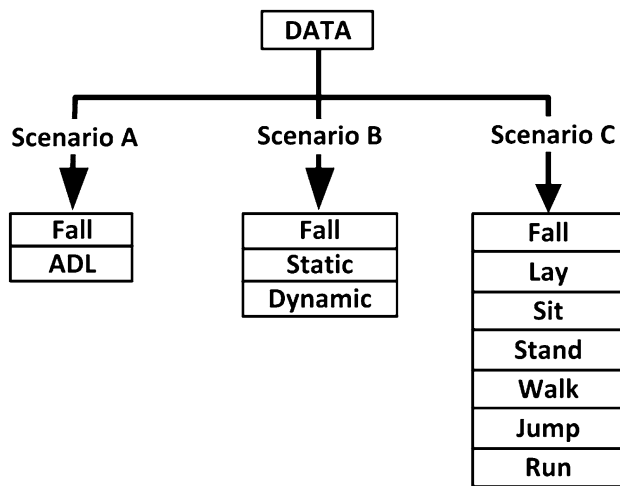


Fig. 3 Proposed scenarios for system evaluation

4.1 Results without CS

Table 5 shows the accuracy performance of the resulting systems relying on the Accelerometer (ACC) and Gyroscope (GYR) sensors, where the results are arranged according to the previously explained scenarios. As shown in Table 5, in general, the gyroscope-based classification yields a higher performance relative to that of the accelerometer, regardless of the used algorithm. When considering a low number of classes, whether two or three, the system is able to achieve an accuracy performance ranging from 99.2 to 99.7% for scenario A, and from 99% to 99.5% for scenario B. Nevertheless, the accuracy performance in the case of scenario C is significantly altered compared to the previous scenarios, more particularly with the gyroscope sensor. We believe that this performance loss is due to the fact that a higher variation in the acceleration than in the angular velocity is involved

with the chosen movements, thereby making the gyroscope less able to discriminate between the movements included in the higher number of classes.

This remark is consolidated by the performance of the system in such a case, when adopting the accelerometer, which is seen to be less sensitive to the variation of the number of the classes and their corresponding movements. Note that, while retaining different variants of Tree and EC algorithms with ACC brings an accuracy improvement in scenario C relative to using GYR, opting for simple type and SD version for Tree and EC algorithms, respectively, see the least gain. To remedy to this limitation in case of scenario C and enhance the system performance from the different metrics point of view, the relative data originating from the two sensors ACC and GYR are concatenated and processed as a unique file mixing the benefits of both sensors. Table 6 lists the achieved performance of the merged ACC and GYR system built by resorting to the 10-fold CV rule, for scenario B. This comparison is carried out from the accuracy (Acc), specificity (Spe), precision (Pre), recall (Rec) and F-score considerations, for A, B and C scenarios. It can be first seen from this table and Fig. 4, that the Acc metric, which was previously evaluated in Table 5 and through the pertaining discussion in a single sensor case, reflects a considerable gain in this case, where the accelerometer and the gyroscope are jointly used, whatever is the considered scenario and the classification method. In the same direction, the graphs in Fig. 4, compare the Acc performance of the original unique-sensor-based and dual-sensors systems, for each scenario. The results illustrated in these graphs confirm the efficiency of the sensors cooperation in enhancing the fall detection scheme and the quality of the classification, regardless of the scenario. In the case of the scenario A, the average achieved accuracies are 99.3%, 99.5%, and 99.7%, for the accelerometer, the gyroscope, and the dual systems, respectively. Similarly, with the same metric, the values of 99.2%, 98.5%,

Table 5 Comparisons of the accuracy of the system for different sensors and different scenarios

	Type	2 class		3 class		7 class	
		ACC	GYR	ACC	GYR	ACC	GYR
Tree	Com	98.9	99.6	98.8	99	94.1	76.9
	Med	98.9	99.6	98.8	99	92	74.4
	Sim	98.6	99.7	98.8	99.1	77.4	60.8
SVM	Lin	99.5	99.2	99.3	98.6	89.6	77.3
	Qua	99.7	99.7	99.8	99.4	94	81.2
	Cub	99.8	99.7	99.7	99.5	95.1	81.2
k-NN	Euc	99.7	99.8	99.6	99.3	94.2	75.6
	Cos	99.2	99.7	99.2	99.4	90.5	73.5
EC	SD	99.4	98.8	99.3	93	86.6	82.7
	BT	99.3	99.6	99.4	99.4	97	64.7

Bold values indicate the highest accuracy rate for each classification algorithm and scenario for different sensors

and 99.6% for scenario B, and 91%, 74.83% and 92% for scenario C are provided. Common to the three scenarios, k-NN and SVM-based systems yield the best stable Acc outcomes.

4.2 Results with CS

For the evaluation of the proposed system incorporating CS, the dataset was divided such that the 80% of the data amount was dedicated to training the classifiers. The remaining 20% of the data, pertaining to the test part, undergoes CS processing, recovery and is subsequently used, for testing the trained models under the different

scenarios (A, B and C). For the evaluation of the recovery signal quality using CS reconstruction algorithms, the peak signal-to-noise ratio (PSNR) was selected. Figure 5 illustrates, for the x, y, and z axis-ACC acquired data, the original signal and the reconstructed ones with different number of iterations. Similarly, Fig. 6 compares the attained PSNR-performance in terms of the number of iterations, of MP and OMP algorithms. The reported results demonstrate the enhancement of the signal recovery accuracy with the increase of the number of iterations, and the efficiency of OMP in yielding a better reconstruction quality in less iterations than MP counterpart.

Table 6 System performance for scenario B

	Type	Acc	Spe	Pre	Rec	F-score
Tree	Com	99.7	99.7	99.7	99.7	99.7
	Med	99.7	99.7	99.7	99.7	99.7
	Sim	99.7	99.7	99.5	99.5	99.5
SVM	Lin	99.2	99.8	99.2	99.2	99.1
	Qua	99.8	99.8	99.7	99.7	99.7
	Cubic	99.8	99.8	99.7	99.7	99.7
k-NN	Euc	99.6	99.6	99.5	99.5	99.5
	Cos	99.7	99.7	99.6	99.6	99.6
EC	SD	99.6	99.7	99.5	99.5	99.5
	BT	99.7	99.7	99.7	99.7	99.7

Bold values indicate the highest accuracy rate for each classification algorithm and scenario for different sensors

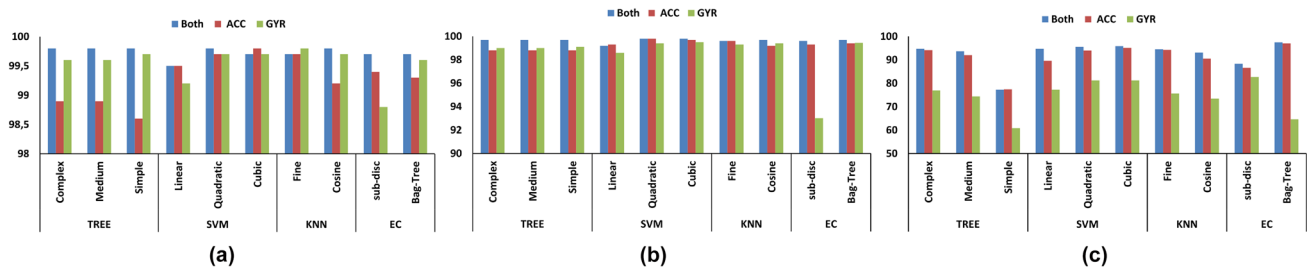


Fig. 4 Obtained results of scenarios with different sensors, **a** Scenario A, **b** Scenario B, **c** Scenario C

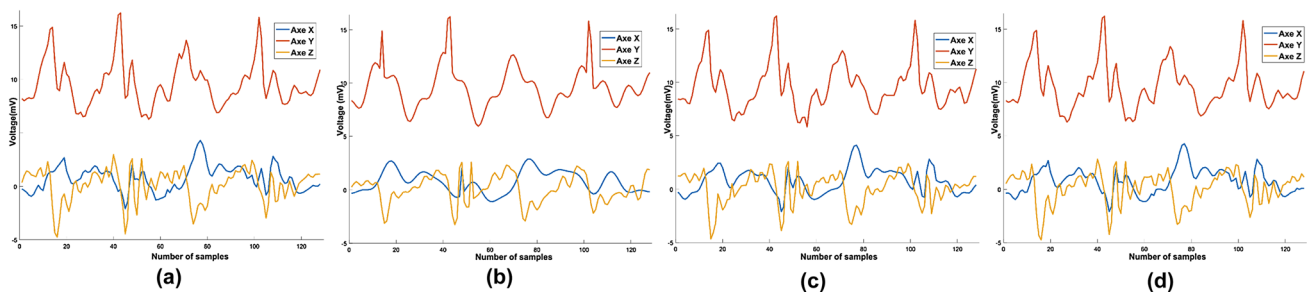


Fig. 5 Comparison between the original and recovery signals using OMP, **a** original signal with ACC, **b** recovery signal after 10 iterations, **c** recovery signal after 30 iterations, **d** recovery signal after 50 iterations

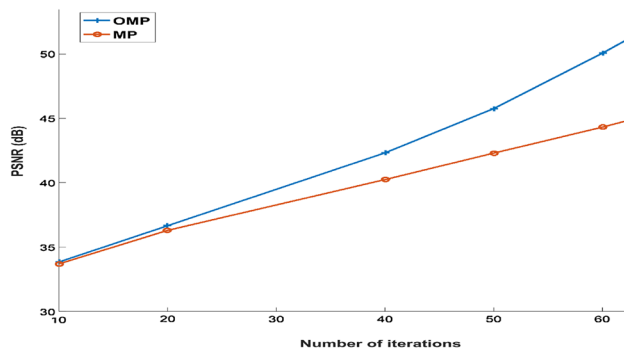


Fig. 6 Comparison between MP and OMP algorithm in terms of PSNR

Table 7 Time execution of MP and OMP approaches with different iterations

Number of Iterations	MP (s)	OMP (s)
10	0.009951	0.073493
20	0.01062	0.09731
30	0.010715	0.135657
50	0.011044	0.141414

Reducing computational complexity is of utmost importance in any practical system, and in inserting the CS processing into the proposed system, this should be carefully observed. To highlight this, Table 7 summarizes the execution time of both MP and OMP algorithms with different iterations. As it can be noted from this table, MP induces less additional time than OMP because of its lower complexity, nonetheless both approaches exhibit reasonable computational complexity.

Table 8 scrutinizes, when embedding CS in the system, the accuracy performance of the dual-sensors CS scheme against the ACC-based alternative. It is seen that, when using a unique sensor, the system relying on OMP approach exhibits the best performance, compared to MP technique, except for the case of 7 classes, where a close behavior is noted with MP and OMP-based schemes. On the other hand, the dual-sensing CS-based system, in scenarios A and B, outperforms the unique-sensor architecture, with the adoption of SVM and EC classification approaches. Figure 7 illustrates the performance variation of these schemes with different classifiers and increased number of iterations in the context of scenario C. As reported in Table 8 and Fig. 7, the architecture relying on OMP algorithm allows to achieve a slightly better performance compared to MP-based counterpart. Furthermore, whereas the impingement of the number of iterations is negligible when resorting to tree classifiers, the performance enhancement with the iterations increase is otherwise noticeable, more particularly, when opting for SVM and KNN alternatives. Finally, SVM and Tree classifiers provide the best fall detection efficiency.

Based on this study, it is clear that no significant penalty is noted with CS processing since the performances of the schemes with and without CS are close. However, the CS-based architectures are more viable since CS aims at ensuring the energy efficiency of the system and increasing the battery life. In our case, we are processing original blocks of data of 128×3 length at once, where the value 3 corresponds to the three signals x , y , and z , which are reduced via CS to 3×50 -long samples; hence, the compression ratio is 61%, a value we obtain through the following relation:

$$\omega = \frac{S_{org} - S_{CS}}{S_{org}} \times 100 \quad (3)$$

Table 8 Performance of the system applying CS at the data

Type		Matching pursuit						Orthogonal matching pursuit					
		ACC			ACC + GYR			ACC			ACC+GYR		
		2class	3class	7class	2class	3class	7class	2class	3class	7class	2class	3class	7class
Tree	Com	95.8	97.5	79	96.4	97.8	78.5	96.1	98.9	79.0	95.3	98	78.2
	Med	95.8	97.5	78.7	96.4	97.8	79.3	96.1	98.9	78.7	95.3	98	79.3
	Sim	98.9	99.1	77.6	98.6	98.3	77.6	98	99.1	77.6	98.3	98.3	77.6
SVM	Lin	99.4	99.7	81.5	100	99.72	91.1	99.4	99.7	81.5	99.7	99.72	91.4
	Qua	99.7	99.7	79.6	99.4	100	89.2	99.7	99.7	78.2	99.7	100	89.5
	Cub	99.7	99.7	77.9	98.9	100	85.4	99.7	99.7	77.4	99.4	100	87.05
k-NN	Euc	100	100	80.4	99.4	99.7	83.4	100	100	79.8	99.7	99.4	85.4
	Cos	99.4	99.4	85.9	99.4	99.4	87.0	99.4	99.4	85.4	99.4	99.4	85.4
EC	SD	98.3	98.6	83.4	100	100	93.1	98.6	98.6	83.4	99.4	100	93.9
	BT	99.1	97.5	79.6	99.4	98.9	91.7	99.1	99.4	79.3	99.4	98.9	91.7

Bold values indicate the highest accuracy rate for each classification algorithm and scenario for different sensors

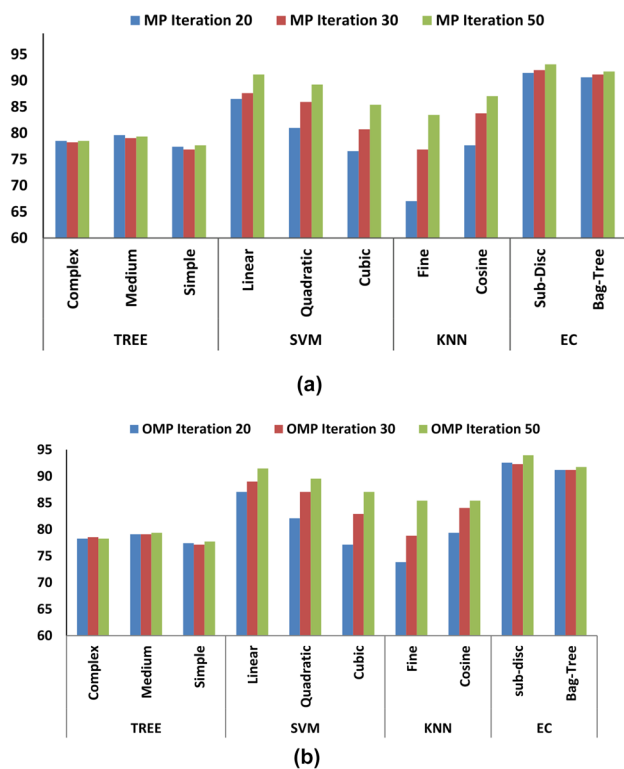


Fig. 7 Performance of the system using CS in scenario C for different iterations, **a** Recovery using MP, **b** recovery using OMP

In real-world usage, it was reported by Gibson et al. (Gibson et al 2017) that standard Bluetooth data streaming performed with the accelerometer sensor of a Shimmer device, at a sampling rate of 50 Hz, requires an average current consumption of 15.9 mA, leading to 17.6 h usage on the

standard 280 mAh battery of the Shimmer devices. Taking into consideration the compression ratio attained by the CS techniques, the resulting offered transmission space saving of 76% would provide 45.05 h of usage under the worst case scenario.

The last table presents a comparison between the classical and the proposed systems against the ones presented in different and recent research studies, in terms of Acc, or Pre. The upper part of Table 9 corresponds to the schemes which do not involve CS in their operation, and their corresponding Acc, number of used sensors and number of classes are provided. Similarly, the lower part compares CS-based approaches where the interest was focused either on the detection of the fall or another movement, along with the offered Rec and Pre. The systems retained for comparison purposes use different devices types and numbers (camera, audio, accelerometer, Kinect) and different classification approaches. However, in carrying out the comparison the same evaluation criteria were selected. In fact, the aim of the comparison was to judge the overall and relative performance of the proposed system in regards to fall detection problem. As it can be noted from this table, the choice of the sensing devices, the number of sensors, their locations and the classification methods, have their impact on the reliability of the system. Furthermore, with CS, only one type of sensor was favoured, and mostly it was the accelerometer. The benefit of resorting to a dual-sensing system with CS is highlighted with our architecture, since superior accuracy and precision performances are attained, compared to the state-of-the-art studies.

Despite the good performance of our system under the specified conditions, for our system to encompass realistic scenarios, it needs to enrich the dataset by adding

Table 9 Performance of different methods without CS

	Ref	Device	Classes	Acc (%)	Pre (%)
Without CS	Aslan et al. (2015)	Depth camera	6	64.67	-
	Aslan et al. (2015)	3 camera	2	97.92	-
	Cheffena (2016)	Audio	2	98	-
	Gibson et al. (2016)	ACC	3	95.3	-
	Gibson et al. (2016)	ACC	5	92.9	-
	Gao et al. (2014)	(1–6) ACC	5	96.4	-
	Our work	ACC/GYR	2	99.8	-
	Our work	ACC/GYR	3	99.8	-
	Our work	ACC/GYR	7	97.2	-
With CS	Cheng et al. (2017a)	4 ACC	5	96.1	96
	Gibson et al. (2017)	ACC	Fall	96	99
	Gibson et al. (2017)	ACC	Strength	91	99
	Gibson et al. (2017)	ACC	Direction	87	98
	Our work	ACC/GYR	2	100	100
	Our work	ACC/GYR	3	100	100
	Our work	ACC/GYR	7	93.9	94

more participants with more movements of elderly people in an unsupervised configuration. Furthermore, since our approach is tested only on shimmer device, tests on other devices are necessary for a viable validation. It is necessary to investigate what kinds of activities are prone to misclassification with the other activities. Figure 4 depicts the obtained results for the three scenarios (A, B and C) and Table 6 showcases the metrics performance for the recognition result for scenario B. Based on these results, almost no misclassifications can be observed, all performance measures are clearly above 99%. Therefore, this result could indicate that daily activity recognition is an easily solvable classification problem, even with a simple classifier such as a decision tree. However, based on the obtained results for scenario C, we observe that the system may confuse between sitting and standing or Jumping and jogging activities and misclassify certain activities. For scenario A and scenario B, the system achieves higher accuracy rates for two classes (fall and no fall) and 3 classes; fall, activity and no activity respectively, where the different classes were correctly classified. The mean class dependent classification rates of sitting and standing were rather low compared to lying and walking. It is assumed that instances of sitting were misclassified as standing and vice versa, which is confirmed by observations in the confusion matrix.

The result depicted on Fig. 4 has two main drawbacks: it is subject dependent (thus does not tell anything about the performance of the system when used by a new subject), and only applies to the specific scenario of these 7 basic activity classes. Therefore, an extension of this result is required to increase the applicability of the system concerning both limitations. Furthermore, it may be noted that we have not considered all classes of activities in daily life in this study. More exhaustive work needs to be carried out in the future to meet more complex activity recognition requirements by a wider range of people, such as aged, young, injured or disabled people. In order to reduce the misclassification, specialized gait features might improve the results for the ADL system recognition. Nevertheless, given the flexibility of the proposed classification system, the incorporation of these ideas is straightforward.

5 Conclusion

This work presents a novel fall and human activity detection system; which incorporates wearable devices for the required body signals acquisition and transmission, their submission to compressed sensing techniques, and their classification, for their subsequent exploitation in ADL-fall recognition process, which keeps in mind the reduction of energy consumption. The system is based on the exploitation of the accelerometer and gyroscope sensors of the

Shimmer platform, and its performance has been examined under three different aspects, i.e. the variation of the scenario (number of classes), the sensor types, and the use or not of the CS techniques.

Regarding the considered scenario, the system was first evaluated for its capability in identifying a fall or a non-fall in scenario (A). The second scenario (B), in addition to the a fall investigation, aimed at detecting if the patient was performing an activity or not. The last scenario (C) attempted to predict six movements, while also detecting falls. All these scenarios were tested and the system's evaluation was carried out under them, using several classification algorithms (k-NN, SVM, DT, EC), and exploiting selected temporal features extracted from the GYR and ACC recordings. The performance of the system was examined for both individual sensors, and the dual-sensors architectures. Experimental results showed that the proposed system which utilizes the whole data-length, achieves an increased performance in terms of accuracy, reaching 99.8% for scenarios A and B, and 97.2% for scenario C, when the dual-sensors scheme is used, instead of the one involving a unique sensor.

After establishing the feasibility of the proposed approach merging the benefits of both sensors, the advantage of incorporating the CS approach was evaluated in order to achieve a reduced power consumption for the Shimmer platform, while ensuring a high accuracy. The performances of the two widely-adopted MP and OMP CS algorithms were studied by scrutinizing the impact of a specific parameter, namely the number of iterations in the CS algorithms, in addition to the ones which were previously investigated (variations of the scenarios, the type of sensors, and the classification methods). Results showed that when retaining the CS methods, an increased battery life was achieved while the accuracy of the system did not suffer. As a result, the adoption of the CS methods in the proposed system was demonstrated to allow a continuous monitoring of the subjects for approximately $2.55 \times$ higher duration (45.05 h vs 17.6 h), as compared to the data full-length approach, thereby indicating that the use of CS is highly beneficial.

Compliance with ethical standards

Conflict of interest The authors declare that they have no conflict of interest.

References

- Alhimale L, Zedan H, Al-Bayatti A (2014) The implementation of an intelligent and video-based fall detection system using a neural network. *Appl Soft Comput* 18:59–69. <https://doi.org/10.1016/j.asoc.2014.01.024>

- Ando B, Baglio S, Lombardo CO, Marletta V (2016) A multisensor data-fusion approach for adl and fall classification. *IEEE Trans Instrum Meas* 65(9):1960–1967. <https://doi.org/10.1109/TIM.2016.2552678>
- Aslan M, Sengur A, Xiao Y, Wang H, Ince MC, Ma X (2015) Shape feature encoding via fisher vector for efficient fall detection in depth-videos. *Appl Soft Comput* 37(C):1023–1028. <https://doi.org/10.1016/j.asoc.2014.12.035>
- Burns A, Doheny E, Greene B, Foran T, Leahy D, O'Donovan K, McGrath M (2010a) An extensible platform for physiological signal capture. In: Engineering in medicine and biology society (EMBC), 2010 annual international conference of the IEEE, pp 3759–3762. <https://doi.org/10.1109/IEMBS.2010.5627535>
- Burns A, Greene BR, McGrath MJ, O'Shea TJ, Kuris B, Ayer SM, Stroiescu F, Cionca V (2010) A wireless sensor platform for non-invasive biomedical research. *IEEE Sens J* 10(9):1527–1534. <https://doi.org/10.1109/JSEN.2010.2045498>
- Candes E, Wakin M (2008) An introduction to compressive sampling. *Signal Process Mag IEEE* 25(2):21–30. <https://doi.org/10.1109/MSP.2007.914731>
- Candes E, Romberg J, Tao T (2006) Robust uncertainty principles: exact signal reconstruction from highly incomplete frequency information. *Inf Theory IEEE Trans* 52(2):489–509. <https://doi.org/10.1109/TIT.2005.862083>
- Casilari E, Santoyo-Ramón JA, Cano-García JM (2017) Analysis of public datasets for wearable fall detection systems. *Sensors* 17(7):1513. <https://doi.org/10.3390/s17071513>
- Cheffena M (2016) Fall detection using smartphone audio features. *IEEE J Biomed Health Inf* 20(4):1073–1080. <https://doi.org/10.1109/JBHI.2015.2425932>
- Cheng L, Guan Y, Zhu K, Li Y (2017a) Recognition of human activities using machine learning methods with wearable sensors. In: 2017 IEEE 7th annual computing and communication workshop and conference (CCWC), pp 1–7. <https://doi.org/10.1109/CCWC.2017.7868369>
- Cheng L, Li Y, Guan Y (2017b) Human activity recognition based on compressed sensing. In: 2017 IEEE 7th annual computing and communication workshop and conference (CCWC), pp 1–7. <https://doi.org/10.1109/CCWC.2017.7868489>
- Cheng L, Li Y, Guan Y (2017c) Human activity recognition based on compressed sensing. In: 2017 IEEE 7th annual computing and communication workshop and conference (CCWC), pp 1–7. <https://doi.org/10.1109/CCWC.2017.7868489>
- Daher M, Diab A, Najjar MEBE, Khalil MA, Charpillat F (2017) Elder tracking and fall detection system using smart tiles. *IEEE Sens J* 17(2):469–479. <https://doi.org/10.1109/JSEN.2016.2625099>
- Donoho DL (2006) Compressed sensing. *IEEE Trans Inf Theor* 52(4):1289–1306. <https://doi.org/10.1109/TIT.2006.871582>
- Duda R, Hart P, Stork D (2012) Pattern classification. Wiley, Oxford
- Feng G, Mai J, Ban Z, Guo X, Wang G (2016) Floor pressure imaging for fall detection with fiber-optic sensors. *IEEE Pervas Comput* 15(2):40–47. <https://doi.org/10.1109/MPRV.2016.27>
- Gao L, Bourke A, Nelson J (2014) Evaluation of accelerometer based multi-sensor versus single-sensor activity recognition systems. *Med Eng Phys* 36(6):779–785
- Ghanem K (2013) Effect of channel correlation and path loss on average channel capacity of body-to-body systems. *IEEE Trans Antenn Propag* 61(12):6260–6265. <https://doi.org/10.1109/TAP.2013.2283035>
- Gibson RM, Amira A, Ramzan N, de la Higuera PC, Pervez Z (2016) Multiple comparator classifier framework for accelerometer-based fall detection and diagnostic. *Appl Soft Comput* 39:94–103. <https://doi.org/10.1016/j.asoc.2015.10.062>
- Gibson RM, Amira A, Ramzan N, de la Higuera PC, Pervez Z (2017) Matching pursuit-based compressive sensing in a wearable biomedical accelerometer fall diagnosis device. *Biomed Signal Process Control* 33:96–108. <https://doi.org/10.1016/j.bspc.2016.10.016>
- Hall KIGKPS (2016) Advances in Body-Centric Wireless Communication: applications and state-of-the-art, Institution of Engineering and Technology, chap Diversity and MIMO for efficient front-end design of body-centric wireless communications devices
- Han J, Qian C, Wang X, Ma D, Zhao J, Xi W, Jiang Z, Wang Z (2016) Twins: Device-free object tracking using passive tags. *IEEE/ACM Trans Netw* 24(3):1605–1617. <https://doi.org/10.1109/TNET.2015.2429657>
- Harrou F, Zerrouki N, Sun Y, Houacine A (2017) Vision-based fall detection system for improving safety of elderly people. *IEEE Instrum Meas Mag* 20(6):49–55. <https://doi.org/10.1109/MIM.2017.8121952>
- Hui S, Zhongmin W (2017) Compressed sensing method for human activity recognition using tri-axis accelerometer on mobile phone. *J China Univ Posts Telecommun* 24(2):31–71. [https://doi.org/10.1016/S1005-8885\(17\)60196-1](https://doi.org/10.1016/S1005-8885(17)60196-1)
- Igual R, Medrano C, Plaza I (2013) Challenges, issues and trends in fall detection systems. *BioMed Eng OnLine* 12(1):66. <https://doi.org/10.1186/1475-925X-12-66>
- Jokanovic B, Amin M, Ahmad F (2016) Radar fall motion detection using deep learning. In: 2016 IEEE radar conference (RadarConf), pp 1–6. <https://doi.org/10.1109/RADAR.2016.7485147>
- Kerdjadj O, Ghanem K, Amira A, Harizi F, Chouireb F (2014) Concatenation of dictionaries for recovery of ecg signals using compressed sensing techniques. In: 2014 26th international conference on microelectronics (ICM), pp 112–115. <https://doi.org/10.1109/ICM.2014.7071819>
- Kwolk B, Kepski M (2016) Fuzzy inference-based fall detection using kinect and body-worn accelerometer. *Appl Soft Comput* 40:305–318. <https://doi.org/10.1016/j.asoc.2015.11.031>
- Lee RYW, Carlisle AJ (2011) Detection of falls using accelerometers and mobile phone technology. *Age Age* 40(6):690–696. <https://doi.org/10.1093/ageing/afr050>
- Li Q, Stankovic JA, Hanson MA, Barth AT, Lach J, Zhou G (2009) Accurate, fast fall detection using gyroscopes and accelerometer-derived posture information. In: 2009 sixth international workshop on wearable and implantable body sensor networks, pp 138–143. <https://doi.org/10.1109/BSN.2009.46>
- Litvak D, Zigel Y, Gannot I (2008) Fall detection of elderly through floor vibrations and sound. In: 2008 30th annual international conference of the IEEE engineering in medicine and biology society, pp 4632–4635. <https://doi.org/10.1109/IEMBS.2008.4650245>
- Lusardi MM (2017) Determining risk of falls in community dwelling older adults: a systematic review and meta-analysis using posttest probability. *J Geriatr Phys Ther* 40:1–36
- Makhlouf A, Boudouane I, Saadia N, Ramdane Cherif A (2018) Ambient assistance service for fall and heart problem detection. *J Amb Intell Hum Comput* 2018:1–20. <https://doi.org/10.1007/s12652-018-0724-4>
- Mallat S, Zhang Z (1993) Matching pursuits with time-frequency dictionaries. *Signal Process IEEE Trans* 41(12):3397–3415. <https://doi.org/10.1109/78.258082>
- Micucci D, Mobilio M, Napoletano P, Tisato F (2017) Falls as anomalies? an experimental evaluation using smartphone accelerometer data. *J Amb Intell Hum Comput* 8(1):87–99. <https://doi.org/10.1007/s12652-015-0337-0>
- Mubashir M, Shao L, Seed L (2013) A survey on fall detection: Principles and approaches. *Neurocomputing* 100:144–152. <https://doi.org/10.1016/j.neucom.2011.09.037>
- Ntanasis P, Pippa E, Özdemir AT, Barshan B, Megalooikonomou V (2017) Investigation of sensor placement for accurate fall detection. Springer, Cham, pp 225–232. <https://doi.org/10.1007/978-3-319-58877-3-30>

- Ozcan K, Velipasalar S, Varshney PK (2017) Autonomous fall detection with wearable cameras by using relative entropy distance measure. *IEEE Trans Hum Mach Syst* 47(1):31–39. <https://doi.org/10.1109/THMS.2016.2620904>
- Ozdemir AT (2016) An analysis on sensor locations of the human body for wearable fall detection devices: Principles and practice. *Sensors* 16(8):1161. <https://doi.org/10.3390/s16081161>
- Ruan W, Sheng QZ, Yao L, Gu T, Ruta M, Shangguan L (2016) Device-free indoor localization and tracking through human-object interactions. In: 2016 IEEE 17th international symposium on a world of wireless, mobile and multimedia networks (WoW-MoM), pp 1–9. <https://doi.org/10.1109/WoWMoM.2016.7523524>
- Sheltami TR, Bala A, Shakshuki EM (2016) Wireless sensor networks for leak detection in pipelines: a survey. *J Amb Intell Hum Comput* 7(3):347–356. <https://doi.org/10.1007/s12652-016-0362-7>
- Sherrington C, Tiedemann A (2017) Physiotherapy in the prevention of falls in older people. *J Physiother* 61:54–60. <https://doi.org/10.1016/j.jphys.2015.02.011>
- Sigg S, Scholz M, Shi S, Ji Y, Beigl M (2013) Rf-sensing of activities from non-cooperative subjects in device-free recognition systems using ambient and local signals. *IEEE Trans Mob Comput* 13:907–920. <https://doi.org/10.1109/TMC.2013.28>
- Tropp JA, Gilbert AC (2005) Signal recovery from partial information via orthogonal matching pursuit. *IEEE Trans Inf Theory* 53:4655–4666
- Tropp JA, Gilbert AC (2007) Signal recovery from random measurements via orthogonal matching pursuit. *IEEE Trans Inf Theory* 53:4655–4666
- Vallabh P, Malekian R (2018) Fall detection monitoring systems: a comprehensive review. *Journal of Ambient Intelligence and Humanized Computing* 9(6):1809–1833. <https://doi.org/10.1007/s12652-017-0592-3>
- Yao L, Sheng QZ, Li X, Wang S, Gu T, Ruan W, Zou W (2015) Freedom: Online activity recognition via dictionary-based sparse representation of rfid sensing data. In: 2015 IEEE international conference on data mining, pp 1087–1092. <https://doi.org/10.1109/ICDM.2015.102>
- Yao L, Sheng QZ, Li X, Gu T, Tan M, Wang X, Wang S, Ruan W (2018) Compressive representation for device-free activity recognition with passive rfid signal strength. *IEEE Trans Mob Comput* 17(2):293–306. <https://doi.org/10.1109/TMC.2017.2706282>
- Zerrouki N, Harrou F, Sun Y, Houacine A (2016) Accelerometer and camera-based strategy for improved human fall detection. *J Med Syst* 40(12):284. <https://doi.org/10.1007/s10916-016-0639-6>
- Zhang S, Feng R, Wu Y, Yu N (2017) Adaptive compressed sensing for acceleration data transmission in human motion capture. In: 2017 10th international congress on image and signal processing, biomedical engineering and informatics (CISP-BMEI), pp 1–6. <https://doi.org/10.1109/CISP-BMEI.2017.8302268>

Publisher's Note Springer Nature remains neutral with regard to jurisdictional claims in published maps and institutional affiliations.